energy&fuels

pubs.acs.org/EF

Communication

Cellulose Degradation by Infrared Free Electron Laser

Takayasu Kawasaki,* Takeshi Sakai, Heishun Zen, Yoske Sumitomo, Kyoko Nogami, Ken Hayakawa, Toyonari Yaji, Toshiaki Ohta, Koichi Tsukiyama, and Yasushi Hayakawa

Cite This: https://dx.doi.org/10.1021/acs.energyfuels.0c01069

Read Online

ACCESS | Metrics & More | Article Recommendations | Supporting Information

ABSTRACT: We introduce a green approach to obtain glucose and low-molecular-weight saccharides directly from the cellulose aggregate by using near- and mid-infrared free electron lasers (IR-FELs). The IR-FEL is a synchrotron radiation based picosecond pulse laser where the oscillation wavelengths are tunable from 3 to 10 μm. Electrospray ionization mass spectroscopy analysis showed that mass peaks of glucose (203 Da), cellobiose (365 Da), trisaccharide (527 Da), and tetrasaccharide (689 Da) were clearly detected as each sodium ion adduct in the soluble fraction after the powdered cellulose was serially irradiated by the IR-FEL tuned to 9.1 μm (νC−O) following 7.2 μm (δH−C−O) or 3.5 μm (νC−H). The production yields of these saccharides were higher than those obtained by the single irradiation at 9.1 μm, as shown by the mass chromatogram analysis. The cleavage of the glucoside bonds was revealed by synchrotron radiation infrared microscopy analysis: the infrared absorption peak of the C−O bonds at 1100 cm^{-1} was obviously reduced, and the bandwidth of the broad peak of O−H bonds at 3400 cm^{-1} was shortened after those irradiations. The laser irradiation system suggested herein is based on the vibration mode selective multiphoton absorption reaction and requires no cosolvents and no high temperatures and pressures to exert the irradiation effect. One day of operation can process several hundred milligrams of the solid cellulose sample at the current laboratory scale.

1. INTRODUCTION

During recent decades, bioethanol production is an urgent issue to realize the oil-removal society. Cellulose and the conjugate with lignin are the most abundant biomass in the earth, and the processing of those carbohydrates is one of the methods for producing biofuels.[1−3] The degradation products, glucose, xylose, and their sugar-alcohol derivatives, can be useful as the carbon source of bacteria fermenting ethanol.[4−6] In addition, cellulose nanofibers are attracting attention as functional biomaterials such as biocompatible cell membranes, antibacterial sheets, and hybrid paper materials in healthcare, pharmaceutical, and engineering industry fields.[7−9] Therefore, the processing technique of the cellulose fibers can be expected as a promising tool for producing low-molecular-weight sugars and recycling the rigid biopolymers. However, the cellulose structure is highly constructed by oligomeric saccharides and is generally undissolved in water.[10−12] To dissolve the polymer, microwave, hydrolysis using ionic liquids, ultrasonication, enzymes of microorganisms, and metal catalysis are developed by chemists and biotechnologists around the world today.[13−18] Nonetheless, each of these approaches has advantages and disadvantages in terms of versatility and conversion efficiency, and further construction of environmentally friendly systems is strongly desired for the zero-emission technology.

In the current study, we propose a novel green process for degradation of cellulose to obtain low-molecular-weight sugars by using an infrared free electron laser (IR-FEL). The IR-FEL is generated by strong interaction of synchrotron radiation (SR) with the accelerated electron beam in the periodic magnetic field (refs 19−21; the outline of the laser system is shown in section 1.2 and Figure S1 in the Supporting Information). In principle, the oscillation wavelengths range widely from near- to far-infrared rays (3−100 μm) and with various wavelengths that can resonate with many functional groups, and the collective vibrational modes are contained in those infrared regions. This feature enables us to perform multiphoton absorption and dissociation reactions by state-selective vibration excitation on various biomolecules.[22−25] As shown in the SR-infrared microscopy (IRM) spectrum of the cellulose fibril (Figure 1a), there are three bands at 9.1, 7.2, and 3.5 μm. These bands can be assigned to the C−O stretching mode (νC−O), H−C−O bending mode (δH−C−O), and C−H stretching mode (νC−H) around the acetal carbon in the polysaccharides (Figure 1b), respectively.[26] The IR-FEL was tuned to those wavelengths and irradiated to the cellulose fibril in a glass bottle at room temperature under atmosphere. After the irradiation, we analyzed the irradiation products by using electrospray ionization mass spectroscopy (ESI-MS) and SR-IRM (the experimental details are described in sections 1.3 and 1.4 in the Supporting Information).

2. RESULTS AND DISCUSSION

2.1. ESI-MS Analysis. The mass profiles of the non-irradiated sample (a) and samples after irradiation at 9.1 μm following 7.2 μm (b) and 3.5 μm (c) are shown in Figure 2. Clearly, there were many peaks detected after irradiation

Received: April 3, 2020
Revised: May 7, 2020
Published: May 8, 2020

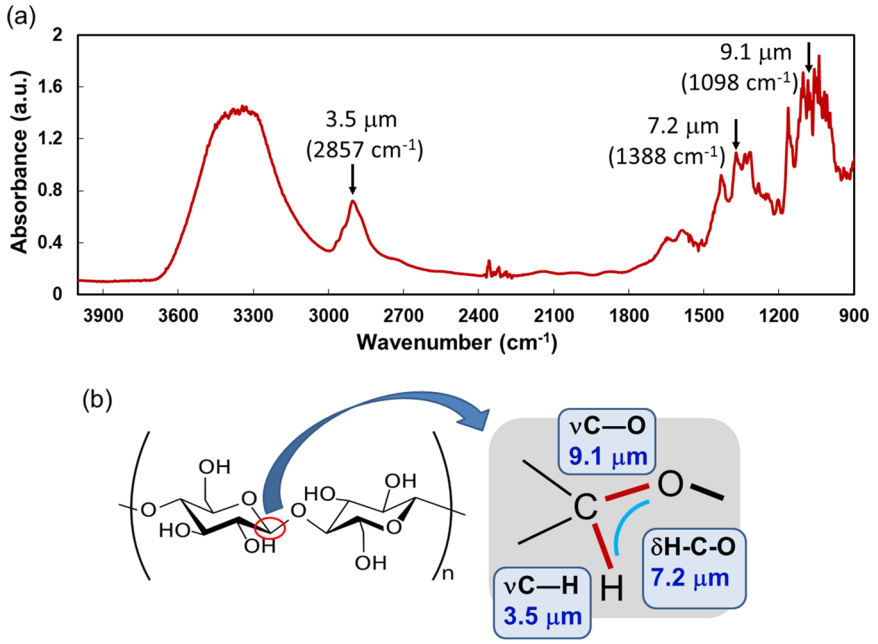

Figure 1. (a) SR-IRM spectrum of cellulose powder. Arrows indicate the target wavelengths for IR-FEL. The original spectrum is shown in section 2.1 in the Supporting Information. (b) Glucoside bonds and resonant wavelengths for νC−O (9.1 μm), δH−C−O (7.2 μm), and νC−H (3.5 μm).

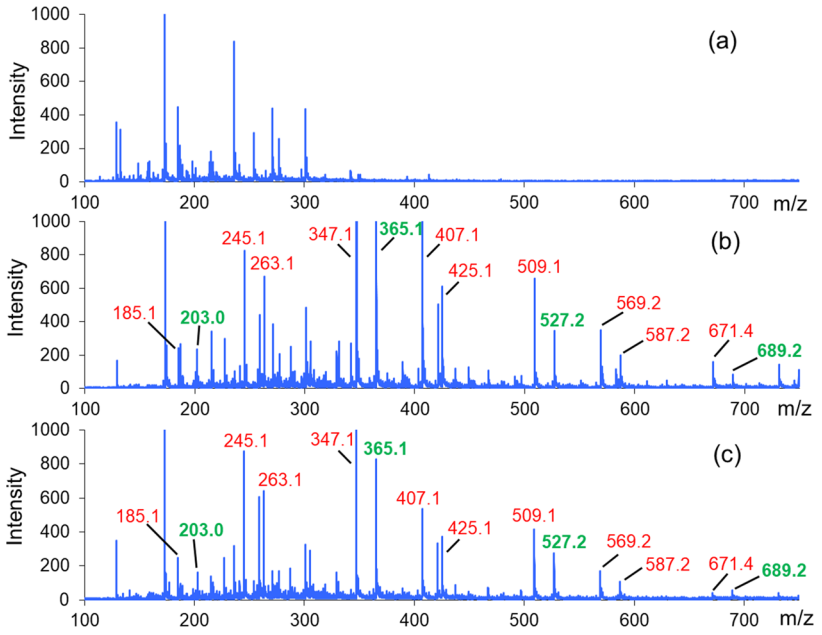

Figure 2. ESI-MS profiles of nonirradiation (a), after serial irradiation at 9.1 μm following 7.2 μm (b), and after serial irradiation at 9.1 μm following 3.5 μm (c). Green numbers indicate mono-, di-, tri-, and tetrasaccharides, in descending order.

compared to the case without irradiation, which indicates that these irradiations caused structural fragmentation of the cellulose aggregate. Interestingly, in both profiles after irradiation, mass peaks at 203.0, 263.1, 365.1, 425.1, 527.2, 587.2, and 689.2 were detected accompanied by each dehydration product (−18 Da), and those mass peaks were not detected in the nonirradiation sample (the original spectral data are shown in section 2.2 in the Supporting Information). Dehydration is usually observed in the electrospray ionization mass measurement of compounds containing the hydroxy groups. In addition, 689.2, 527.2, 365.1, and 203.0 Da can be assigned to tetrasaccharide, trisaccharides, cellobiose, and glucose as each sodium ion adduct, respectively. Therefore, not only mono- and disaccharides but also the oligomeric sugars were derived from the cellulose aggregate by the laser irradiation. The mass differences between 203.1 and 263.1, 365.1 and 425.1, and 527.2 and 587.2 were all 60 Da that can correspond to CH_3CO_2H, which indicates the sample employed here contains monoacetylated sugars.

Next, we estimated the yields of cellobiose and glucose by mass chromatography analysis. The soluble fraction of the cellulose powder after being suspended in water was eluted in the liquid chromatography column (Figure 3). In the case of single irradiation at 9.1 μm (red), both ion peaks of cellobiose (left) and glucose (right) were obviously detected compared to the case of nonirradiation (black). Interestingly, the serial

https://dx.doi.org/10.1021/acs.energyfuels.0c01069
Energy Fuels XXXX, XXX, XXX−XXX

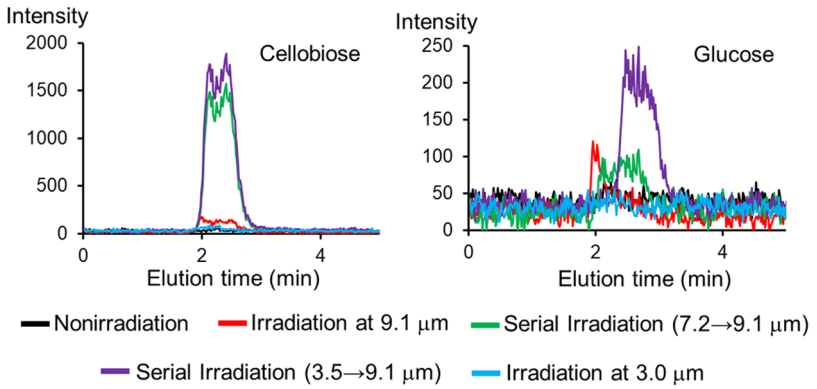

Figure 3. Mass chromatograms of cellobiose (left) and glucose (right) before the laser irradiation (black) and after the irradiation at 9.1 μm (red), 9.1 μm following 7.2 μm (green), 9.1 μm following 3.5 μm (violet), and 3.0 μm (blue). Each mass peak was detected as a sodium ion adduct, 365 Da for cellobiose and 203 Da for glucose.

irradiation at 9.1 μm following 3.5 μm (violet) and 7.2 μm (green) afforded more cellobiose, and the irradiation following 3.5 μm was most effective for production of glucose. The production yield was calculated to be about 1% for cellobiose and about 0.2% for glucose based on the total ion peak intensity. The irradiation at 3.0 μm (blue) that corresponds to the O−H stretching mode was not effective for production of those saccharides. This implies that the glucoside bond was not affected by the activation of the hydroxy group.

2.2. SR-IRM Analysis. In the SR-IRM spectra (Figure 4), the C−O stretch vibrational bands of cellulose were observed

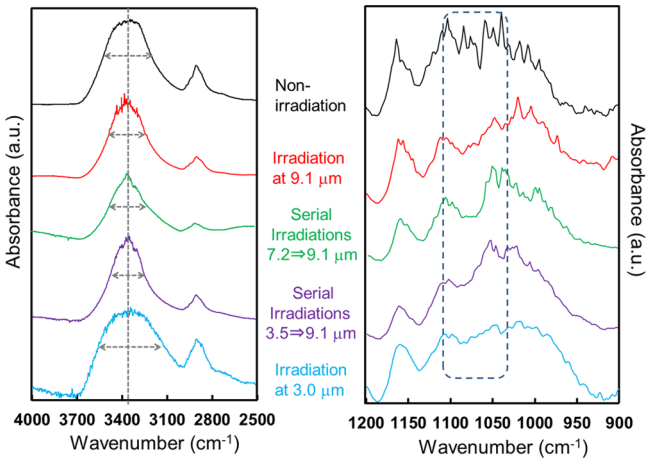

Figure 4. SR-IRM spectra of cellulose aggregates before laser irradiation (black) and after irradiation at 9.1 μm (red), 9.1 μm following 7.2 μm (green), 9.1 μm following 3.5 μm (violet), and 3.0 μm (blue). Left, near-infrared region; right, mid-infrared region. Double-headed arrow: half width of the infrared absorption peak.

from 1000 to 1150 cm^{-1} (right panel), and several peaks from 1050 to 1100 cm^{-1} in the nonirradiation sample (black) correspond to glucoside bonds, which were assigned by comparison of the spectrum of cellobiose having one glucoside bond with that of glucose having no glucoside bond (the spectral data are shown in section 2.1 of the Supporting Information). After irradiation at 9.1 μm (red), 9.1 μm following 7.2 μm (green), and 9.1 μm following 3.5 μm (violet), this region was clearly concave compared to the nonirradiation (black) and irradiation at 3.0 μm (blue) samples, as indicated by a gray dotted frame. In the near-infrared region (left panel), the O−H stretching band was observed as broad band at around 3400 cm^{-1} (gray dotted line). The half width (as indicated by a double-headed arrow) was about 350 cm^{-1} for the nonirradiation sample (black) and 400 cm^{-1} for the sample after irradiation at 3.0 μm (blue). On the contrary, all three irradiations at 9.1 μm (red), 9.1 μm following 7.2 μm (green), and 9.1 μm following 3.5 μm (violet) shortened the half width to about 300 cm^{-1}. These spectral changes in the hydroxy group region mean that those irradiations except for 3.0 μm drastically changed the structure of cellulose from the nonirradiation sample. Together with the spectral change in the mid-infrared region, it is certain that the irradiations targeting the acetal group caused the dissociation of the glucoside bonds in the cellulose. We also observed the morphological change of the cellulose fibril after irradiation at 9.1 μm following 3.5 μm by using scanning electron microscopy (SEM). The fiberlike structure was substantially destroyed and dispersed into the short fragments by the irradiation (the images are shown in Figure S2 of the Supporting Information).

2.3. Insight into the Laser-Induced Degradation Mechanism. It should be noted that the vibrational excitation at the C−H stretching mode and H−C−O bending mode prior to the excitation at the C−O stretching mode are remarkably effective for production of glucose and cellobiose from the cellulose aggregate (Scheme 1). In the theoretical

Scheme 1. Production of Glucose and Cellobiose from Cellulose by Means of Infrared Free Electron Laser Irradiation

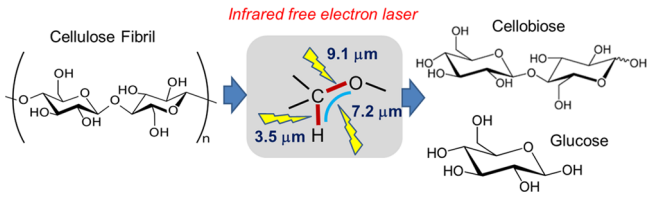

study using nonequilibration simulation,[27] the laser irradiation at 1360 cm^{-1} that resonates with the C3−O3−H3 bending vibrational mode can disrupt the hydrogen bond network in the aggregate structure of cellulose. The bundle of carbohydrate polymers can be dissociated to free chains after 10 ns irradiation. A similar dissociation mechanism was proposed by a nonequilibrium simulation of peptide nanotubes.[28] None-

https://dx.doi.org/10.1021/acs.energyfuels.0c01069
Energy Fuels XXXX, XXX, XXX−XXX

theless, the cleavage of covalent bonds such as C−O bonds was unclear in those studies. We first observed that the serial irradiation at 9.1 μm following 7.2 μm was more effective for the cleavage of the glucoside bonds than the single irradiation at 9.1 μm. Therefore, the vibrational excitation at the H−C−O bending mode can unravel the fibril structure and thereby the naked glucoside bonds are easily dissociated by the multiphoton absorption reaction at C−O stretching vibrational mode. Interestingly, the excitation of C−H bonds (3.5 μm) afforded more amounts of glucose than the case of 7.2 μm (Figure 3). In the cellulose aggregate, intermolecular hydrogen bonds between H2−O6 have important roles for fiber formation.[27] It can be considered that the vibrational excitation at 3.5 μm can disrupt the interchain hydrogen bonds and is more effective for dissociation of the fibril structure of the cellulose than the irradiation at 7.2 μm. This is a novel finding, and the activation of C−H bonds by the infrared laser will be applied to the structural alteration of other biomass materials such as lignin in future studies.

2.4. Feature of the Method. This physical method using IR-FEL needs no specific conditions such as acidic or alkaline solutions, organic solvents, high pressures, and high temperatures.[29−31] One more important point that we should suggest is that both glycoside bond cleavage and dissociation of the hydrogen bonds in the stacked carbohydrate chains can be achieved in a one batch system by selecting the wavelength, and the laser-induced dissociation reaction can proceed within several hundred picoseconds due to the pulse structure of the free electron laser.[32,33] These features have an advantage over the conventional system using microbial enzymes in terms of the rapidness and simplicity.[34,35] However, the production yield of the glucose by using IR-FEL was comparatively low at the present laboratory scale (milligram level). Therefore, a successive irradiation system such as a continuous supply of samples to the beamline should be developed for the mass production of glucose at the gram scale. Nonetheless, securing the utility expenses for the maintenance of the laser system is a significant issue. Regarding the practical aspect of the process for the degradation of cellulose, commercially available enzymes such as cellulase may be superior to the laser system. The present study first showed the primitive conditions such as optimal wavelengths for degradation of cellulose by using the IR-FEL to produce glucose and low-molecular-weight saccharides. In the future, a compact-size and low-cost operation system that possesses the same oscillation parameters as the IR-FEL should be developed for the practical use.

3. CONCLUSION

We performed laser degradation of cellulose aggregates by tuning the wavelength of an infrared free electron laser to 9.1 μm (νC−O) following 7.2 μm (δH−C−O) and 3.5 μm (νC−H). ESI-MS and SR-IRM analyses showed that the glucoside bonds were cleaved and glucose and cellobiose accompanied by the low-molecular-weight oligomeric sugars were produced by the irradiation. This laser system can be operated at room temperature under atmosphere and requires no cosolvents. It can be expected that the use of IR-FEL contributes to a green process for the production of glucose from carbohydrate biomass.

■ ASSOCIATED CONTENT

Supporting Information

The Supporting Information is available free of charge at https://pubs.acs.org/doi/10.1021/acs.energyfuels.0c01069.

Experimental details, FT-IR spectra, ESI-MS data, and SEM images (PDF)

■ AUTHOR INFORMATION

Corresponding Author

Takayasu Kawasaki − *IR-FEL Research Center, Research Institute for Science and Technology, Organization for Research Advancement, Tokyo University of Science, Noda, Chiba 278-8510, Japan*; orcid.org/0000-0001-8376-5807; Email: kawasaki@rs.tus.ac.jp

Authors

Takeshi Sakai − *Laboratory for Electron Beam Research and Application (LEBRA), Institute of Quantum Science, Nihon University, Funabashi, Chiba 274-8501, Japan*

Heishun Zen − *Institute of Advanced Energy, Kyoto University, Uji, Kyoto 611-0011, Japan*

Yoske Sumitomo − *Laboratory for Electron Beam Research and Application (LEBRA), Institute of Quantum Science, Nihon University, Funabashi, Chiba 274-8501, Japan*

Kyoko Nogami − *Laboratory for Electron Beam Research and Application (LEBRA), Institute of Quantum Science, Nihon University, Funabashi, Chiba 274-8501, Japan*

Ken Hayakawa − *Laboratory for Electron Beam Research and Application (LEBRA), Institute of Quantum Science, Nihon University, Funabashi, Chiba 274-8501, Japan*

Toyonari Yaji − *SR Center, Research Organization of Science and Technology, Ritsumeikan University, Kusatsu, Shiga 525-8577, Japan*

Toshiaki Ohta − *SR Center, Research Organization of Science and Technology, Ritsumeikan University, Kusatsu, Shiga 525-8577, Japan*

Koichi Tsukiyama − *IR-FEL Research Center, Research Institute for Science and Technology, Organization for Research Advancement, Tokyo University of Science, Noda, Chiba 278-8510, Japan*

Yasushi Hayakawa − *Laboratory for Electron Beam Research and Application (LEBRA), Institute of Quantum Science, Nihon University, Funabashi, Chiba 274-8501, Japan*

Complete contact information is available at: https://pubs.acs.org/10.1021/acs.energyfuels.0c01069

Notes

The authors declare no competing financial interest.

■ ACKNOWLEDGMENTS

We thank the technical staff of Tokyo University of Science for mass spectroscopy measurements. This work was supported in part by the Open Advanced Research Facilities Initiative and Photon Beam Platform Project of the Ministry of Education, Culture, Sports, Science and Technology of Japan, the collaborative research with SR Center of Ritsumeikan University (Subject Number: S19001 in 2019), the "Joint Usage/Research Program on Zero-Emission Energy Research, Institute of Advanced Energy, Kyoto University (ZE31A-12)", and collaborative research with LEBRA at Nihon university.

https://dx.doi.org/10.1021/acs.energyfuels.0c01069
Energy Fuels XXXX, XXX, XXX−XXX

REFERENCES

(1) Zheng, J.; Rehmann, L. Extrusion pretreatment of lignocellulosic biomass: a review. *Int. J. Mol. Sci.* **2014**, *15*, 18967−18984.

(2) Linde, M.; Galbe, M.; Zacchi, G. Bioethanol production from non-starch carbohydrate residues in process streams from a dry-mill ethanol plant. *Bioresour. Technol.* **2008**, *99*, 6505−6511.

(3) Gumina, B.; Espro, C.; Galvagno, S.; Pietropaolo, R.; Mauriello, F. Bioethanol Production from Unpretreated Cellulose under Neutral Selfsustainable Hydrolysis/Hydrogenolysis Conditions Promoted by the Heterogeneous Pd/Fe3O4 Catalyst. *ACS Omega* **2019**, *4*, 352−357.

(4) Nijland, J. G.; Driessen, A. J. M. Engineering of Pentose Transport in Saccharomyces cerevisiae for Biotechnological Applications. *Front. Bioeng. Biotechnol.* **2020**, *7*, 464.

(5) Laluce, C.; Schenberg, A. C.; Gallardo, J. C.; Coradello, L. F.; Pombeiro-Sponchiado, S. R. Advances and developments in strategies to improve strains of Saccharomyces cerevisiae and processes to obtain the lignocellulosic ethanol–a review. *Appl. Biochem. Biotechnol.* **2012**, *166*, 1908−1926.

(6) Li, J.; Zhang, Y.; Li, J.; Sun, T.; Tian, C. Metabolic engineering of the cellulolytic thermophilic fungus Myceliophthora thermophila to produce ethanol from cellobiose. *Biotechnol. Biofuels* **2020**, *13*, 23.

(7) Hong, S.; Sunwoo, J. H.; Kim, J. S.; Tchah, H.; Hwang, C. Conjugation of carboxymethyl cellulose and dopamine for cell sheet harvesting. *Biomater. Sci.* **2019**, *7*, 139−148.

(8) Baruah, S.; Jaisai, M.; Imani, R.; Nazhad, M. M.; Dutta, J. Photocatalytic paper using zinc oxide nanorods. *Sci. Technol. Adv. Mater.* **2010**, *11*, No. 055002.

(9) Zhang, M.; Wu, X.; Hu, Z.; Xiang, Z.; Song, T.; Lu, F. A Highly Efficient and Durable Fluorescent Paper Produced from Bacterial Cellulose/Eu Complex and Cellulosic Fibers. *Nanomaterials* **2019**, *9*, 1322.

(10) Moon, R. J.; Martini, A.; Nairn, J.; Simonsen, J.; Youngblood, J. Cellulose nanomaterials review: structure, properties and nanocomposites. *Chem. Soc. Rev.* **2011**, *40*, 3941−3994.

(11) El Seoud, O. A.; Kostag, M.; Jedvert, K.; Malek, N. I. Cellulose in Ionic Liquids and Alkaline Solutions: Advances in the Mechanisms of Biopolymer Dissolution and Regeneration. *Polymers (Basel, Switz.)* **2019**, *11*, 1917.

(12) Lee, C. M.; Kubicki, J. D.; Fan, B.; Zhong, L.; Jarvis, M. C.; Kim, S. H. Hydrogen-Bonding Network and OH Stretch Vibration of Cellulose: Comparison of Computational Modeling with Polarized IR and SFG Spectra. *J. Phys. Chem. B* **2015**, *119*, 15138−15149.

(13) Delbecq, F.; Len, C. Recent Advances in the Microwave-Assisted Production of Hydroxymethylfurfural by Hydrolysis of Cellulose Derivatives-A Review. *Molecules* **2018**, *23*, 1973.

(14) Froschauer, C.; Hummel, M.; Iakovlev, M.; Roselli, A.; Schottenberger, H.; Sixta, H. Separation of hemicellulose and cellulose from wood pulp by means of ionic liquid/cosolvent systems. *Biomacromolecules* **2013**, *14*, 1741−1750.

(15) Guo, X.; Shang, X.; Zhou, X.; Zhao, B.; Zhang, J. Ultrasound-assisted extraction of polysaccharides from Rhododendron agganiphum: Antioxidant activity and rheological properties. *Ultrason. Sonochem.* **2017**, *38*, 246−255.

(16) Minty, J. J.; Singer, M. E.; Scholz, S. A.; Bae, C. H.; Ahn, J. H.; Foster, C. E.; Liao, J. C.; Lin, X. N. Design and characterization of synthetic fungal-bacterial consortia for direct production of isobutanol from cellulosic biomass. *Proc. Natl. Acad. Sci. U. S. A.* **2013**, *110*, 14592−14597.

(17) Manaenkov, O. V.; Kislitsa, O. V.; Matveeva, V. G.; Sulman, E. M.; Sulman, M. G.; Bronstein, L. M. Cellulose Conversion Into Hexitols and Glycols in Water: Recent Advances in Catalyst Development. *Front. Chem.* **2019**, *7*, 834.

(18) Van de Vyver, S.; Geboers, J.; Schutyser, W.; Dusselier, M.; Eloy, P.; Dornez, E.; Seo, J. W.; Courtin, C. M.; Gaigneaux, E. M.; Jacobs, P. A.; Sels, B. F. Tuning the acid/metal balance of carbon nanofiber-supported nickel catalysts for hydrolytic hydrogenation of cellulose. *ChemSusChem* **2012**, *5*, 1549−1558.

(19) O'Shea, P. G.; Freund, H. P. Free-electron lasers: Status and applications. *Science* **2001**, *292*, 1853−1858.

(20) Zen, H.; Suphakul, S.; Kii, T.; Masuda, K.; Ohgaki, H. Present status and perspectives of long wavelength free electron lasers at Kyoto University. *Phys. Procedia* **2016**, *84*, 47−53.

(21) Kuwada-Kusunose, T.; Kusunose, A.; Wakami, M.; Takebayashi, C.; Goto, H.; Aida, M.; Sakai, T.; Nakao, K.; Nogami, K.; Inagaki, M.; Hayakawa, K.; Suzuki, K.; Sakae, T. Evaluation of irradiation effects of near-infrared free-electron-laser of silver alloy for dental application. *Lasers Med. Sci.* **2017**, *32*, 1349−1355.

(22) Edwards, G. S.; Allen, S. J.; Haglund, R. F.; Nemanich, R. J.; Redlich, B.; Simon, J. D.; Yang, W. C. Application of free-electron lasers in the biological and material sciences. *Photochem. Photobiol.* **2005**, *81*, 711−735.

(23) Boles, G. C.; Hightower, R. L.; Coates, R. A.; McNary, C. P.; Berden, G.; Oomens, J.; Armentrout, P. B. Experimental and Theoretical Investigations of Infrared Multiple Photon Dissociation Spectra of Aspartic Acid Complexes with Zn2+ and Cd2+. *J. Phys. Chem. B* **2018**, *122*, 3836−3853.

(24) Hoang Man, V.; Van-Oanh, N. T.; Derreumaux, P.; Li, M. S.; Roland, C.; Sagui, C.; Nguyen, P. H. Picosecond infrared laser-induced all-atom nonequilibrium molecular dynamics simulation of dissociation of viruses. *Phys. Chem. Chem. Phys.* **2016**, *18*, 11951−11958.

(25) Kawasaki, T.; Tsukiyama, K.; Irizawa, A. Dissolution of a fibrous peptide by terahertz free electron laser. *Sci. Rep.* **2019**, *9*, 10636.

(26) Mazurek, S.; Mucciolo, A.; Humbel, B. M.; Nawrath, C. Transmission Fourier transform infrared microspectroscopy allows simultaneous assessment of cutin and cell-wall polysaccharides of Arabidopsis petals. *Plant J.* **2013**, *74*, 880−891.

(27) Domin, D.; Man, V. H.; Van-Oanh, N.; Wang, J.; Kawasaki, T.; Derreumaux, P.; Nguyen, P. H. Breaking down cellulose fibrils with a mid-infrared laser. *Cellulose* **2018**, *25*, 5553−5568.

(28) Hoang Viet, M.; Truong, P. M.; Derreumaux, P.; Li, M. S.; Roland, C.; Sagui, C.; Nguyen, P. H. Picosecond melting of peptide nanotubes using an infrared laser: a nonequilibrium simulation study. *Phys. Chem. Chem. Phys.* **2015**, *17*, 27275−27280.

(29) Cantero, D. A.; Bermejo, M. D.; Cocero, M. J. Governing chemistry of cellulose hydrolysis in supercritical water. *ChemSusChem* **2015**, *8*, 1026−1033.

(30) Bodachivskyi, I.; Kuzhiumparambil, U.; Williams, D. B. G. High Yielding Acid-Catalysed Hydrolysis of Cellulosic Polysaccharides and Native Biomass into Low Molecular Weight Sugars in Mixed Ionic Liquid Systems. *ChemistryOpen* **2019**, *8*, 1316−1324.

(31) Ooi, B. G.; Rambo, A. L.; Hurtado, M. A. Overcoming the recalcitrance for the conversion of kenaf pulp to glucose via microwave-assisted pre-treatment processes. *Int. J. Mol. Sci.* **2011**, *12*, 1451−1463.

(32) Austin, R. H.; Xie, A.; van der Meer, L.; Redlich, B.; Lindgård, P. A.; Frauenfelder, H.; Fu, D. Picosecond thermometer in the amide I band of myoglobin. *Phys. Rev. Lett.* **2005**, *94*, 128101.

(33) Hutson, M. S.; Ivanov, B.; Jayasinghe, A.; Adunas, G.; Xiao, Y.; Guo, M.; Kozub, J. Interplay of wavelength, fluence and spot-size in free-electron laser ablation of cornea. *Opt. Express* **2009**, *17*, 9840−9850.

(34) Srivastava, N.; Rathour, R.; Jha, S.; Pandey, K.; Srivastava, M.; Thakur, V. K.; Sengar, R. S.; Gupta, V. K.; Mazumder, P. B.; Khan, A. F.; Mishra, P. K. Microbial Beta Glucosidase Enzymes: Recent Advances in Biomass Conversation for Biofuels Application. *Biomolecules* **2019**, *9* (6), 220.

(35) Tozakidis, I. E.; Brossette, T.; Lenz, F.; Maas, R. M.; Jose, J. Proof of concept for the simplified breakdown of cellulose by combining Pseudomonas putida strains with surface displayed thermophilic endocellulase, exocellulase and β-glucosidase. *Microb. Cell Fact.* **2016**, *15*, 103.

https://dx.doi.org/10.1021/acs.energyfuels.0c01069
Energy Fuels XXXX, XXX, XXX−XXX